ARTICLE TYPE

Silver(I) coordination complexes and extended networks assembled from S, Se, Te substituted acenaphthenes

Fergus R. Knight,[*a] **Rebecca R. M. Randall,**[a] **Lucy Wakefield,**[a] **Alexandra M. Z. Slawin,**[a] **and J. Derek Woollins***

Six related organo-chalconium silver(I) coordination complexes, including two examples of rare organotellurium-silver coordination, have been prepared and structurally characterised by X-ray crystallography. The series of 5-bromo-6-(phenylchalcogeno)acenaphthene ligands **L1**-**L3**
[10] [Acenap(Br)(EPh)] (Acenap = acenaphthene-5,6-diyl; E = S, Se, Te) were independently treated with silver(I) salts (AgBF$_4$, AgOTf). In order to keep the number of variables to a minimum, all reactions were carried out using a 1:1 ratio of Ag/L and run in dichloromethane. The nature of the donor atoms and the coordinating ability of the respective counter-anion affects the structural architecture of the final silver(I) complex, generating monomeric, mononuclear, two-coordinate silver(I) complexes {[AgBF$_4$(L)$_2$] (**1** L =
[15] **L1**; **2** L = **L2**; **3** L = **L3**)}, a monomeric three-coordinate silver(I) complex {[AgOTf(**L2**)$_2$] **5**}, a monomeric four-coordinate silver(I) complex {[AgOTf(**L1**)$_3$] **4**} and a 1D extended helical chain polymer {[AgOTf(**L3**)]$_n$ **6**}. The organic acenaphthene ligands **L1**-**L3** all adopt the same ligation mode with the central silver atom (classical monodentate coordination), which employs a variety of coordination geometries (linear, bent, trigonal planar, tetrahedral).

Introduction

[20] Supramolecular coordination networks assembled from tunable ligands and transition metals have recieved great attention due to their intrinsic structural characteristics and applications in polymer design and materials science.[1-6] The archetypical design
[25] utilises bridging organic ligands as ridgid supports to link central metal ions in an ordered lattice, creating extended, multidimensional networks.[4-6] Functionalisation of the ligand shell allows the properties, topology and geometry of the extended network to be tailored, allowing new functional
[30] materials to be developed. As such, the metal-ligand interaction is an important building block for the design and manufacture of organic solids and metal-organic frameworks (MOFs).[4-6]

Control over the polymeric architecture of the network is,
[35] nevertheless a major challenge, governed as it is by additional experimental factors such as the oxidation state of the metal, the coordination geometry, the metal-to-ligand ratio, the nature and spacer length of the bridging ligand, the presence of solvent molecules and the nature of the counter-anions.[4,7] Subtle
[40] modification to any of these parameters can significantly alter the structure of the complexes produced, generating for example classical monomeric, mononuclear species, linear chain polymers or extended three-dimensional networks.[4-6]

[45] The diverse coordination chemistry associated with the Ag(I) ion as a consequence of a 4d^{10} configuration allows for a variety of different coordination geometries to be achieved, thus making silver an attractive and preferred choice of metal for constructing supramolecular networks.[4-6,8] Furthermore, short Ag⋯Ag
[50] contacts between neighbouring metal centres and the greater influence of intermolecular interactions and crystal packing forces associated with a weaker silver-ligand bond contribute to the formation of the extended structure.[5,6,8] Additional benefits of silver over other metals include the ability to simulatneously bind
[55] to hard (O,N)[6,9] and soft (S)[6,10] donor atoms and the availability of a wide range of silver(I) salts, enabling the contribution of the counter-anions in the extended network to be analysed.

The polycyclic aromatic hydrocarbons, naphthalene[11] and related
[60] 1,2-dihydroacenaphthylene (acenaphthene)[12] provide good scaffolds from which to design donor ligands for the construction of metal complexes and extended networks.[13] The double substitution of groups or atoms at the proximal *peri*-positions inevitably increases the degree of steric hindrance within the
[65] molecule as a result of repulsive interactions resulting from sub-van der Waals contacts.[14] This leads to deformation of the carbon frameworks away from their natural geometry via in-plane and out-of-plane distortions and buckling of the aromatic ring system (angular strain). Metal coordination is therefore favoured inorder
[70] to reduce the steric strain and achieve a relaxed geometry without invoking greater molecular distortion.[13] The ability to tune the donor functionalities enables a variety of coordination modes to be accomplished including classical monodentate, bis-

monodentate μ_2-bridging, bidentate chelating and asymmetric hemilabile coordination.[13]
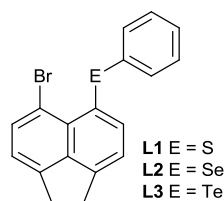

Fig. 1 Acenaphthene bromo-chalcogen donor ligands **L1**-**L3**.[20]

In a combined study of Group 15 and 16 substituted compounds, we have previously utilised the naphthalene backbone to prepare a variety of chalcogen and phosphorus compounds and associated metal complexes.[15-18] More recently we have focused on the acenaphthene skeleton investigating chalcogen-tin[19] compounds and related halogen-chalcogen and chalcogen-chalcogen derivatives.[20] From a recent study, the series of chalcogen-donor ligands Acenap[EPh][E`Ph] (Acenap = acenaphthene-5,6-diyl; E/E` = S, Se, Te) were shown to be ideal building blocks from which to construct coordination networks. Self-assembly with the series of silver(I) salts silver tetrafluoroborate (AgBF$_4$), silver trifluoromethanesulfonate (AgOTf) and silver hexafluorophosphate (AgPF$_6$) afforded a range of 3D metal-organic frameworks, 1D polymeric chains and monomeric, mononuclear silver(I) complexes.[21]

Herein we present a similar structural study of the complexes formed between 5-(bromo)-6-(phenylchalcogeno)acenaphthenes [Acenap(Br)(EPh)] (Acenap = acenaphthene-5,6-diyl; E = S, Se, Te) **L1**-**L3**[20] (Figure 1) and AgBF$_4$ and AgOTf. The nature of the donor atoms and the coordinating ability of the respective counter-anion affects the structural architecture of the final silver(I) complex, generating two- three- and four- coordinate monomeric, mononuclear silver(I) complexes **1**-**5** and a 1D extended helical chain polymer **6**.

Whilst coordination complexes formed between organo-sulfur compounds and silver(I) salts are fairly common, those assembled from organo-selenides and organo-tellurides are much rarer. In fact, at the time of writing, a Cambridge Structural Database (CSD; version 5.33)[22] search yielded only five examples of organo-tellurium silver(I) complexes.[23]

Results and Discussion

The series of acenaphthene bromo-chalcogen donor compounds {[Acenap(Br)(EPh)] (Acenap = acenaphthene-5,6-diyl; E = S, Se, Te) **L1**-**L3**} were each independently treated with silver tetrafluoroborate [AgBF$_4$] and silver trifluoromethanesulfonate [AgOTf]. Reactions were carried out using a 1:1 ratio of Ag/**L** and run in dichloromethane under an oxygen- and moisture-free nitrogen atmosphere. All the complexes obtained (**1**-**6**) were characterised by multinuclear NMR and IR spectroscopy and mass spectrometry and the homogeneity of the new compounds was where possible confirmed by microanalysis; ^{77}Se and [125]Te NMR data can be found in Table 1. Crystal structures were determined for all six compounds, which were found to be unstable towards light whilst in solution. Selected interatomic

distances, angles and torsion angles are listed in Tables 2 and 3. Further crystallographic information including hydrogen-bond and other non-conventioanl weak inter- and intra-molecular interaction data can be found in Tables S1-S3 and Figures S1-S4 in the Electronic Supporting Information (ESI).

Table 1 ^{77}Se and [125]Te NMR spectroscopic data[a]

	L2	2	5	L3	3	6
Peri-atoms	Br,Se	Br,Se	Br,Se	Br,Te	Br,Te	Br,Te
^{77}Se NMR	423.7	390.6	387.8	-	-	-
[125]Te NMR	-	-	-	696.0	562.0	559.0

[a] **2**, **3**, **5** run in (CD$_3$)$_2$CO, **6** run in CD$_3$CN, **L2**, **L3** run in CDCl$_3$; δ (ppm).

[AgBF$_4$(L1)$_2$] 1. Treatment of 5-bromo-6-(phenylsulfanyl)-acenaphthene **L1**[20] with AgBF$_4$ afforded a two-coordinate, monomeric, silver(I) complex [Ag(BF$_4$){Acenap(Br)(SPh)}$_2$] **1** (Figure 2). Crystals suitable for X-ray diffraction were obtained by slow diffusion of hexane into a saturated solution of the product in dichloromethane, at room temperature in the absence of light. The asymmetric unit contains two silver(I) centres, four sulfur-donor **L1** ligands and two tetrafluoroborate counter-anions.
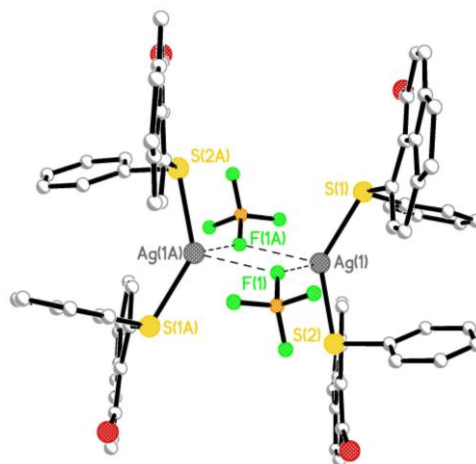

Fig. 2 Two **L1** ligands bind to silver(I) via monodentate sulfur coordination to form complex **1**; two molecules are linked via a central Ag$_2$F$_2$ rhombus core formed from weak Ag···F contacts (H atoms omitted for clarity).

Within the structure, two crystallographically distinct molecules of the sulfur-donor **L1** act as monodentate ligands, binding to silver through S coordination, affording a two-coordinate monomeric complex. The central silver atom adopts a distorted bent coordination geometry, with an obtuse S(1)-Ag(1)-S(2) angle of 137.19(9)°. Additionally, neighbouring molecules of the silver complex link up to form dimers, joined by an Ag$_2$F$_2$ rhombus core formed from weak intermolecular Ag···F interactions [Ag(1)···F(1) 2.511(9) Å; Ag(1)···F(1)^1 2.563(7) Å; Figure 3]. As a consequence of the symmetry the Ag$_2$F$_2$ core is strictly planar in the form of a parallelogram containing two unequal Ag···F bond distances, with the closest non-bonded Ag···Ag distance 4.05 Å. In the secondary coordination sphere, the additional intramolecular Ag(1)···F(1) contacts complete a *quasi*-see-saw coordination geometry around each silver centre (Figure 3).

ARTICLE TYPE

Table 2 Selected interatomic distances [Å] and angles [°] for **1-6**

Compound	1		2	3	4			5		6
Ligand; *peri*-atoms	**L1a**; Br,S	**L1b**; Br,S	**L2**; Br,Se	**L3**; Br,Te	**L1a**; Br,S	**L1b**; Br,S	**L1c**; Br,S	**L2a**; Br,Se	**L2b**; Br,Se	**L3**; Br,Te
Peri-region-distances										
Br···E	3.260(4)	3.263(3)	3.2068(13)	3.2625(12)	3.261(3)	3.281(3)	3.260(3)	3.1427(11)	3.1337(11)	3.222(3)
Σr_{vdW} - Br···E^a; % $\Sigma r_{vdW}{}^a$	0.390; 89	0.387; 89	0.543; 86	0.648; 83	0.389; 89	0.369; 90	0.390; 89	0.607; 84	0.616; 84	0.688; 82
Peri-region bond angles										
Br(1)-C(1)-C(10)	124.5(8)	121.9(8)	122.7(4)	120.7(6)	123.2(9)	124.1(9)	125.1(8)	123.0(4)	122.6(4)	120.8(10)
C(1)-C(10)-C(9)	129.7(13)	134.5(12)	132.6(5)	133.2(7)	132.8(10)	131.2(10)	130.4(7)	131.0(4)	131.5(5)	131.2(11)
E(1)-C(9)-C(10)	122.1(10)	121.6(10)	121.7(4)	123.3(6)	123.5(6)	123.9(6)	124.8(6)	122.0(4)	121.4(4)	124.3(8)
Σ of bay angles	376.3(18)	378.0(18)	377.0(8)	377.5(11)	379.5(15)	379.2(15)	380.3(12)	376.0(7)	375.5(8)	376.3(17)
Splay angle^b	16.3	18.0	17.0	17.5	19.5	19.2	20.3	16.0	15.5	16.3
Out-of-plane displacement										
Br	-0.306(1)	-0.190(1)	0.135(1)	0.101(1)	-0.277(1)	-0.030(1)	0.166(1)	-0.020(1)	0.091(1)	0.039(1)
E	0.554(1)	0.379(1)	0.122(1)	-0.187(1)	0.147(1)	0.353(1)	0.109(1)	0.140(1)	-0.084(1)	0.196(1)
Central naphthalene ring torsion angles										
C:(6)-(5)-(10)-(1)	176.29(1)	172.60(1)	179.67(1)	178.92(1)	-177.59(1)	178.51(1)	179.02(1)	178.63(1)	176.86(1)	-178.33(1)
C:(4)-(5)-(10)-(9)	173.60(1)	177.40(1)	178.35(1)	179.43(1)	178.61(1)	177.31(1)	178.05(1)	-177.63(1)	177.56(1)	177.78(1)

^{a} van der Waals radii used for calculations: r_{vdW}(Br) 1.85Å, r_{vdW}(S) 1.80Å, r_{vdW}(Se) 1.90Å, r_{vdW}(Te) 2.06Å;[24] ^{b}Splay angle: Σ of the three bay region angles – 360.

Coordination to silver has no significant effect on the conformation of the acenaphthene components or the degree of molecular distortion occurring within the organic framework compared with the parent donor ligand **L1**.[20] The two independent acenaphthene fragments (**L1a**/**L1b**) adopt similar axial conformations;[25] in each case aligning the S-C$_{Ph}$ bond perpendicular to the organic backbone corresponding to a type A configuration[26] [Br···S-C$_{Ph}$ angle: **L1a** 84.2°; **L1b** 84.3°], with the bulk of the phenyl moiety directed away from the central Ag$_2$F$_2$ rhombus core.
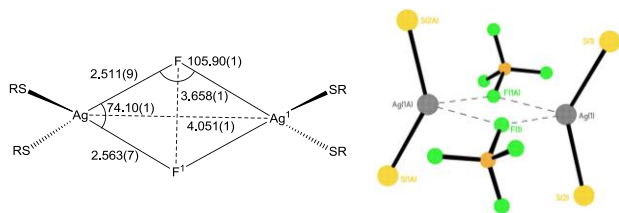

Fig. 3 A schematic representation of the Ag$_2$F$_2$ rhombus core; SR = [Acenap(Br(SPh)], bond distances [Å], angles [°]

The non-bonded intramolecular Br1···S1 distances [**L1a** 3.260(4) Å; **L1b** 3.263(3) Å] are 11% shorter than the sum of the van der Waals radii for the two *peri*-atoms and comparable to the free ligand **L1** (3.297(3) Å).[20] Whilst there is a minor decrease in the degree of in-plane distortion [splay angle: **L1a** 16.3°; **L1b** 18.0°; *cf.* **L1** 20.3°], this is compensated for by an increase in the displacement of the two *peri*-atoms from the mean acenaphthene plane [**L1a**/**L1b** 0.2-0.6 Å; *cf.* **L1** ~0.1 Å].[20] Additionally, there is a notable increase in the buckling of the organic framework of both acenaphthene components, with maximum C-C-C-C central
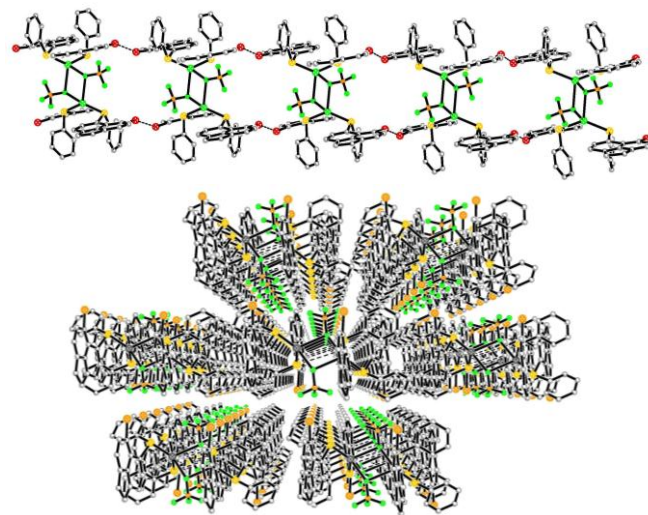
torsion angles 3-7° (*cf.* **L1** 1-3°).[20]

Fig. 4 Neighbouring molecules of **1** connect via weak Br···Br interactions forming extended chains (top) which pack in parallel columns (bottom)

Dimer molecules of **1** assemble in parallel columns and are linked by weak intermolecular Br(1)···Br(2) (3.428 Å) and C(19)-Br(2)···cg(13-18) (3.99 Å) interactions to form extended chains (Figure 4). Within each chain, the planar Ag$_2$F$_2$ rhombus cores stack to form layers, separated by 10.29 Å. Adjacent chains interact via weak CH···π interactions [C(15)-H(15)···cg(5-10) 2.96 Å] and short C(29)-H(29)···S(1) contacts (2.85 Å), with the BF$_4^-$ counter-anions lying in holes between adjacent acenaphthene frameworks.

ARTICLE TYPE

Table 3 Selected silver coordination interatomic distances [Å] and angles [°] for **1-6**

1				**2**		**3**	
Ag(1)-S(1)	2.481(4)	**S(1)-Ag(1)-S(2)**	137.19(9)	**Ag(1)-Se(1)**	2.5596(13)	**Ag(1)-Te(1)**	2.6572(9)
Ag(1)-S(2)	2.488(3)	**S(1)-Ag(1)-F(1)**	109.79(1)	**Ag(1)···Br(1)**	3.2506(12)	**Ag(1)···Br(1)**	3.4993(12)
Ag(1)···F(1)	2.511(9)	**S(1)-Ag(1)-F(1)[1]**	108.60(1)	**Se(1)-Ag(1)-Se(1)[1]**	167.37(3)	**Te(1)-Ag(1)-Te(1)[1]**	167.68(5)
Ag(1)···F(1)[1]	2.563(7)	**S(2)-Ag(1)-F(1)**	97.81(1)	**Se(1)-Ag(1)-Br(1)**	65.75(1)	**Te(1)-Ag(1)-Br(1)**	62.24(1)
Ag(1)···Ag(1)[1]	4.051(1)	**S(2)-Ag(1)-F(1)[1]**	110.13(1)	**Se(1)-Ag(1)-Br(1)[1]**	108.15(1)	**Te(1)-Ag(1)-Br(1)[1]**	111.04(1)
F(1)···F(1)[1]	3.058(1)	**F(1)-Ag(1)-F(1)[1]**	74.10(1)	**Br(1)-Ag(1)-Br(1)[1]**	126.39(3)	**Br(1)-Ag(1)-Br(1)[1]**	120.28(1)
		Ag(1)-F(1)-Ag(1)[1]	105.90(1)	**6**			

4				**6**			
				Ag(1)-Te(1)	2.6714(15)	**Te(1)-Ag(1)-O(1)**	135.04(19)
Ag(1)-S(1)	2.506(3)	**S(1)-Ag(1)-S(3)**	119.05(7)	**Ag(1)-O(1)**	2.377(9)	**Te(1)-Ag(1)-O(2)**	117.62(1)
Ag(1)-S(2)	2.569(3)	**S(2)-Ag(1)-S(3)**	97.73(9)	**Ag(1)···O(2)[2]**	2.469(9)	**Te(1)-Ag(1)-O(3)**	114.75(1)
Ag(1)-S(3)	2.591(3)	**S(1)-Ag(1)-O(1)**	109.2(3)	**Ag(1)···O(3)[1]**	2.778(10)	**O(1)-Ag(1)-O(2)**	81.17(1)
Ag(1)-O(1)	2.395(10)	**S(2)-Ag(1)-O(1)**	96.4(2)	**Ag(1)···O(3)[3]**	2.518(9)	**O(1)-Ag(1)-O(3)**	78.53(1)
S(1)-Ag(1)-S(2)	127.83(9)	**S(3)-Ag(1)-O(1)**	102.0(3)	**Ag(1)···Ag(1)[1]**	3.542(3)	**O(2)-Ag(1)-O(3)**	122.40(1)

5							
Ag(1)-Se(1)	2.5952(9)	**Ag(1)···Br(1)**	3.1921(13)	**Se(1)-Ag(1)-Se(2)**	137.30(3)	**Br(1)-Ag(1)-O(1)**	75.01(1)
Ag(1)-Se(2)	2.5923(9)	**Ag(1)···Br(2)**	3.3524(13)	**Se(1)-Ag(1)-O(1)**	112.81(9)	**Se(2)-Ag(1)-Br(2)**	62.08(1)
Ag(1)-O(1)	2.382(4)	**Se(1)-Ag(1)-Br(1)**	64.82(1)	**Se(2)-Ag(1)-O(1)**	109.88(9)	**Br(2)-Ag(1)-O(1)**	73.54(1)
		Se(1)-Ag(1)-Br(2)	130.53(1)	**Br(1)-Ag(1)-Br(2)**	148.52(1)	**Br(1)-Ag(1)-Se(2)**	129.67(1)

[AgBF₄(L2)₂] 2 & [AgBF₄(L3)₂] 3. Reaction of the corresponding selenium and tellurium analogues [Acenap(Br)(SePh)] **L2**[20] and [Acenap(Br)(TePh)] **L3**[20] with AgBF₄ afforded two isomorphous monomeric two-coordinate silver(I) complexes [Ag(BF₄){Acenap(Br)(EPh)}₂] (**2** E = Se; **3** E = Te; Figure 5). Crystals of **2** suitable for X-ray diffraction were obtained by recrystallization from diffusion of hexane into a saturated acetone solution, whilst crystals of **3** were obtained from hexane/dichloromethane. Recrystallisations of both products were performed at room temperature, in the absence of light to prevent the complexes from decomposing.
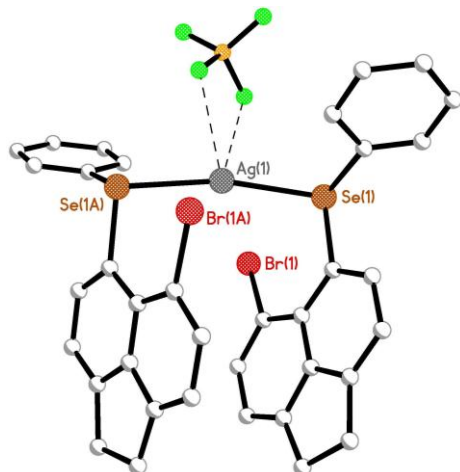

Fig. 5 The two-coordinate mononuclear complex **2** (H atoms omitted for clarity). The structure of **3** (adopting the same configuration) is omitted here but can be found in Figure S1 in the ESI

The nearly identical asymmetric units contain four silver(I) centres, eight chalcogen **L2/L3**[20] ligands and four tetrafluoroborate counter-anions (disordered in **3**). As a consequence of the symmetry (crystallising in the monoclinic C2/c space group) and in contrast with complex **1**, only one crystallographically independent ligand is present in each crystal structure; two crystallographically *identical* molecules of the respective ligand (**L2/L3**) bind with silver, via monodentate E coordination, to afford the monomeric complex [**2** Ag(1)-Se(1) 2.5596(13) Å; **3** Ag(1)-Te(1) 2.6572(9) Å; Figure 5]. The central silver atom adopts a *quasi*-linear coordination geometry with an E(1)-Ag(1)-E(1) angles of 167.37(3) Å (**2** E = Se) and 167.68(5) Å (**3** E = Te). In the secondary coordination sphere, additional intramolecular Ag(1)···Br(1) contacts [**2** 3.2506(12) Å; **3** 3.4993(12) Å], complete a *quasi*-chelate ring with the central silver atom which assumes a distorted see-saw geometry in both complexes [Br(1)-Ag(1)-Br(1)[1] **2** 126.39(3)°; **3** 120.28(1)°; E(1)-Ag(1)-Br(1) **2** 65.75(1)°; **3** 62.24(1)°; E(1)-Ag(1)-Br(1)[1] **2** 108.15(1)°; **3** 111.04(1)°; Figure 6].
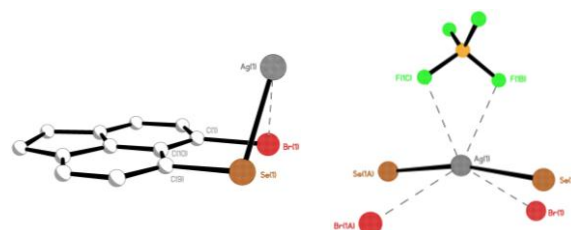

Fig. 6 The open envelope configuration of the *pseudo*-chelate ring formed by weak intramolecular Br···Ag interactions (left) and the central seesaw geometry around Ag(1) afforded by interactions in the secondary coordination sphere. Comparable images of **3** are omitted here but can be found in Figure S2 in the ESI.

The AgBrEC$_3$ six-membered chelate rings subsequently formed adopt twisted envelope type conformations, hinged about the Br···E vectors; Br(1), E(1), C(1), C(9), C(10) are essentially coplanar in each case [mean deviation **2** 0.0371(1) Å; **3** 0.0371(1) Å] with the silver atom sitting in the *peri*-gap, displaced 2.334(1) Å and 2.500(1) Å above this plane respectively, with the Ag(1)-Br(1)-E(1) planes inclined by 101.30(1)° and 100.32(1)° (Figure 6). In both complexes, additional weak intermolecular Ag···F interactions link the silver centre to a single BF$_4^-$ counteranion, positioned directly above the molecule [**2** F(1)···Ag(1) 2.737(4) Å; **3** F(1)···Ag(1) 2.802(6) Å; Figures 5, 6].
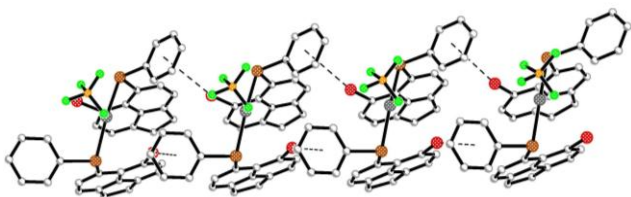

Fig. 7 Complexes **2** and **3** pack along the x-axis with neighbouring molecules linked via weak CBr···π type interactions to form extended chains. Complex **2** shown here, a similar image for **3** can be found in the ESI.

Whilst coordination to silver has no apparent influence on the acenaphthene configurations of either complex (both adopt equatorial arrangements similar to **L2/L3**),[20,25] the *pseudo*-bidentate coordination forces the *peri*-atoms in **2** to lie further apart compared to the free ligand [splay angle: **2** 17.0°; *cf.* **L2** 14.6°],[20] subsequently elongating the non-bonding intramolecular Br(1)···Se(1) *peri*-distance from 3.1588(16) Å in **L2**[20] to 3.2068(13) Å in **2**. Notably less molecular distortion is required to accommodate the silver atom in **3** due to the greater degree of distortion occurring naturally by the presence of the larger tellurium heteroatom; only a minor lengthening of the *peri*-gap is observed compared with the free ligand **L3** [Br(1)···Te(1) **3** 3.2625(12) Å; **L3** 3.2503(11) Å].[20] Nevertheless, both complexes exhibit an increase in the planarity of the organic backbone [maximum C-C-C-C torsion angles: **2/3** 2°; *cf.* **L2/L3** 5°] and a reduction in the displacement of the *peri*-atoms to opposite sides of the mean plane [**2/3** ~0.1 Å; *cf.* **L2** 0.3-0.4 Å].[20]**Error! Bookmark not defined.**
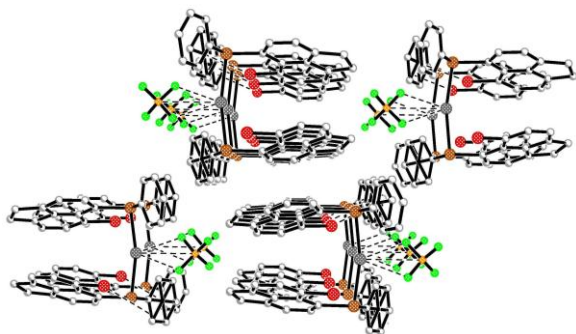

Fig. 8 Packing of complex **2** viewed along the x-axis (H atoms omitted for clarity). A comparable image of **3** can be found in the ESI.

Within the extended structure of both complexes, neighbouring molecules stack along the x-axis and connect via weak intermolecular C-Br···π interactions [C(1)-Br(1)···cg(13-18) **2**

3.64 Å; **2** 3.71 Å] forming extended chains (Figure 7). Silver atoms subsequently align in columns, with the closest Ag···Ag distances between adjacent silver atoms of 7.943(1) Å (**2**) and 7.970(1) Å (**3**). The non-coordinating BF$_4^-$ counter-anions lie in the channels between the acenaphthene moieties and interact with the organic framework via additional CH···F interactions [2.26-2.51 Å; Figure 8].

In contrast to the tetrafluroborate anion, the coordinating ability of the trifluoromethanesulfonate (triflate) counter-anion has a significant impact on the self-assembly of the Acenap(Br)(EPh) donor ligands with AgOTf and dictates the topology and geometric architecture of the final solid state structures.

[AgOTf(L1)$_3$] 4. The reaction between [Acenap(Br)(SPh)] **L1**[20] and AgOTf afforded a four-coordinate, mononuclear silver(I) complex [Ag(OTf){Acenap(Br)(SPh)}$_3$] **4** (Figure 9). Crystals suitable for X-ray diffraction were obtained by recrystallization from diffusion of hexane into a saturated dichloromethane solution of the product in the absence of light, at room temperature. The asymmetric unit of **4** contains two silver(I) centres, six **L1** ligands and two disordered triflate counter-anions.
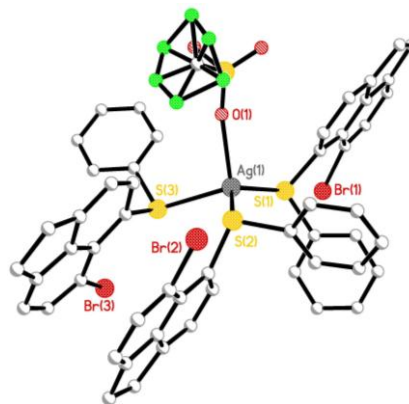

Fig. 9 The four-coordinate mononuclear complex **4** with disordered triflate counter-anion (H atoms omitted for clarity).

In contrast to complex **1**, the capacity of the trifluoromethanesulfonate (triflate) counter-anion to coordinate to silver has a significant impact on the geometry and molecular configuration of the final solid state structure. Three crystallographically distinct molecules of the sulfur-donor ligand (**L1a-L1c**) bind to silver via monodentate S coordination, with an additional Ag-O bond to the coordinating disordered triflate anion completing a distorted tetrahedral geometry around the central silver atom [Ag-S 2.506(3)-2.591(3) Å, Ag-O 2.395(10) Å; S-Ag-S/S-Ag-O 96.4(2)°-127.83(9)°; Figure 9].

The three independent acenaphthene ligands (**L1a-L1c**) each adopt similar axial conformations (type A),[25,26] aligning the S-C$_{Ph}$ bond perpendicular to the mean plane of the organic backbone, with the pheynl rings pointing away from the centre of the molecule. Similar to complex **1**, coordination to silver has a limited impact on the degree of molecular distortion occurring in **L1a-L1c** compared with the free ligand **L1**,[20] with non-bonded intramolecular Br···S distances 3.260(3)-3.281(3) Å compared with 3.297(3) Å in **L1**.[20] Two non-bonded intramolecular CH···F

contacts [C(47)-H(47)···F(5) 2.47 Å; C(48)-H(48)···F(5) 2.45 Å] align the triflate molecule along the mean plane of acenaphthene fragment **L1c** adding extra stability to the structure (Figure 10). Silver centres of neighbouring molecules align in columns along the x-axis, with the closest intermolecular Ag···Ag distance 9.297(1) Å. Adjacent molecules of **4** interact via weak intermolecular C(42)-H(42)···Br(1) interactions (2.91 Å) with further short contacts linking acenaphthene backbones to proximal triflate anions [C(57)-H(57)···F(6) 2.35 Å; C(57)-H(57)···O(3) 2.38 Å].
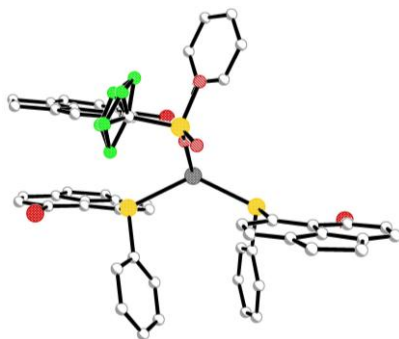

Fig.10 Weak CH···F type interactions align the triflate molecule along the plane of the second acenphthene ring.

[AgOTf(L2)₂] 5. The corresponding reaction between the heavier selenium ligand **L2**[20] with AgOTf afforded a three-coordinate complex [Ag(OTf){Acenap(Br)(SePh)}₂] **5** (Figure 11). Crystals suitable for X-ray diffraction were obtained by recrystallization from diffusion of hexane into a saturated acetone solution of the product at room temperature, in the absence of light. The asymmetric unit contains two silver(I) centres, four selenium **L2** ligands and two coordinating triflate counter-anions.
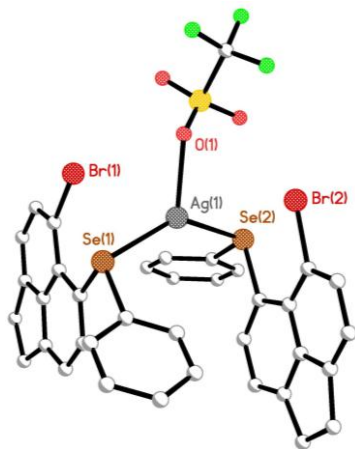

Fig.11 The three-coordinate monomeric, mononuclear complex **5** (H atoms omitted for clarity)

The three-coordinate complex **5** adopts a comparable structure to **2**, with subtle differences accounted for by the coordinating ability of the triflate counter anion. In contrast with **2**, two crystallographically distinct molecules of **L2** bind to the central silver atom via similar monodentate Se coordination [Ag(1)-Se(1) 2.5952(9) Å; Ag(1)-Se(2) 2.5923(9) Å]. The triflate counter-anion occupies a similar position to the BF₄⁻ anion in **2**, however, coordination to silver via a single O atom completes a trigonal

planar geometry around the central metal [Ag(1)-O(1) 2.382(4) Å; Se(1)-Ag(1)-Se(2) 137.30(3) Å; Se(1)-Ag(1)-O(1) 112.81(9) Å; Se(2)-Ag(1)-O(1) 109.88(9) Å; Figure 12].
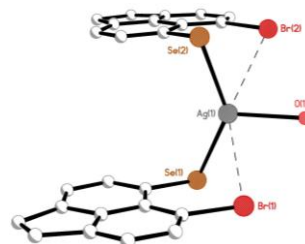

Fig. 12 In the primary coordination sphere the central silver metal adopts a trigonal planar geometry, with supplementary weak Br···Ag contacts completing a trigonal bipyramidal configuration and forming two comparable 6-membered chelate rings (H atoms and phenyl rings omitted for clarity).

To accommodate the change in metal coordination in **5**, rotation around the Ag(1)-Se(2) bond positions the non-bonded Br···Se interaction of **L2b** *quasi*-perpendicular to that of **L2a**, whilst maintaining a parallel alignment of the two acenaphthene backbones (*cf.* **2** the two acenaphthene planes and *peri*-interactions align parallel to one another). The equatorial arrangement adopted by **L2a** and **L2b**,[25] aligning the Se-C_{Ph} bonds along the respective acenaphthene plane, subsequently positions both phenyl rings in close proximity to the neighbouring acenaphthene ring, allowing short intramolecular CH···π interactions to stabilise the molecule [C(14)-H(14)···cg(23-28) 2.90 Å; Figure 12]. The two non-bonded Br···Se distances [**L2a** 3.1427(11) Å; **L2b** 3.1337(11) Å] are comparable to the free ligand **L2** (3.1588(16) Å)[20] suggesting the three-coordinate geometry around silver in **5** has less of an impact on the acenaphthene framework compared with complex **2**.
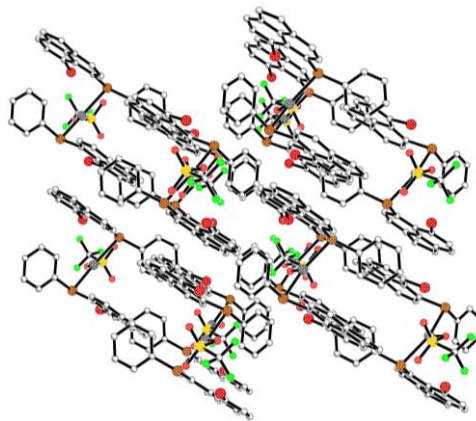

Fig. 13 Weak CH···F and CH···O interactions link triflate molecules to the organic frameworks of neighbouring molecules to form extended chains; packing of **5** as viewed down the y-axis (H atoms omitted for clarity).

Supplementary intramolecular Ag···Br contacts [Ag(1)···Br(1) 3.1921(13) Å; Ag(1)···Br(2) 3.3524(13) Å] allow the two unique **L2** molecules to attain a *quasi*-chelate ring, with the central silver atom assuming a distorted trigonal bipyramidal coordination geometry (Figure 12). The two comparable AgBrSeC₃ six-membered twisted envelope type chelate ring systems hinge about the Br···Se vector; in each case BrSeCCC are virtually

coplanar [mean deviation **L2a** 0.0195(1) Å; **L2b** 0.0321(1) Å] with the silver atom sitting in the *peri*-gap, displaced **L2a** 2.286(1) Å and **L2b** 2.391(1) Å above this plane, with the Ag-Br-Se plane inclined by **L2a** 105.55(1)º and **L2b** 100.66(1)º (Figure 12). Within the extended structure, weak intermolecular CH···π, CF···π, CH···F and CH···O interactions link neighbouring triflate anions and acenaphthene rings to form extended chains which propagate along the y-axis (Figure 13).

[AgOTf(L3)] 6. In stark contrast to the previous complexes, self-assembly of tellurium donor [Acenap(Br)(TePh)] **L3**[20] with AgOTf afforded a mononuclear 1D extended helical chain polymer [Ag(CF$_3$SO$_3$){Acenap(Br)(TePh)}]$_n$ **6** (Figure 14). Crystals suitable for X-ray diffraction were obtained by slow diffusion of hexane into a saturated solution of **6** in tetrahydrofuran, at room temperature in the absence of light. The asymmetric unit contains eight silver(I) centres, eight tellurium **L3** ligands and eight coordinating triflate counter-anions.
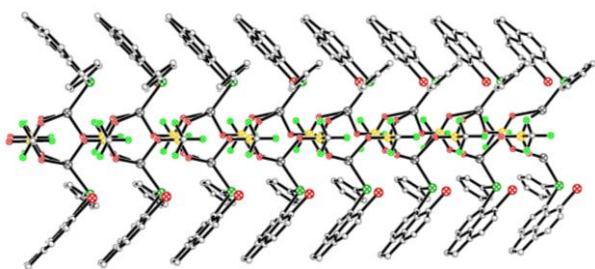
Fig. 14 View of the 1D extended helical chain polymer **6** along the x-axis (H atoms omitted for clarity)

Within the polymeric chain, the monodentate **L3** ligand adopts a similar coordination mode to complexes **1-5**, binding through tellurium to a single silver centre [Ag(1)-Te(1) 2.6714(15) Å; Figure 15]. The simultaneous coordination of four triflate molecules around each silver atom blocks any secondary coordination by additional molecules of **L3**.
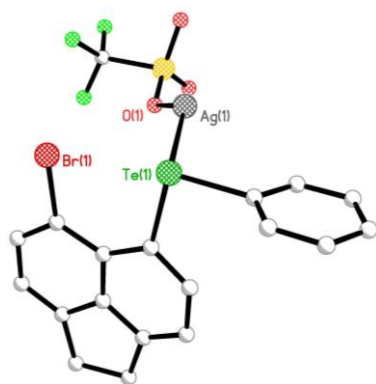
Fig. 15 The repeating unit of extended helical chain polymer **6** (H atoms omitted for clarity)

In the primary coordination sphere, each silver atom coordinates with a single Te atom of an **L3** ligand and an O atom from the closest triflate anion, thus adopting a distorted bent geometry [Ag(1)-O(1) 2.377(9) Å; Te(1)-Ag(1)-O(1) 135.04(19)º; Figure 15]. Three supplementary weak Ag···O interactions link the silver ion to three separate triflate anions generating a distorted see-saw geometry [Ag(1)···O(2)^2 2.469(9) Å; Ag(1)···O(3)^1

2.778(10) Å; Ag(1)···O(3)^3 2.518(9) Å]. Subsequently each triflate molecule, binding through all three O atoms, acts as a linker between four neighbouring silver centres (μ$_4$-bridging) and helps to propagate the extended chain structure (Figure 16).
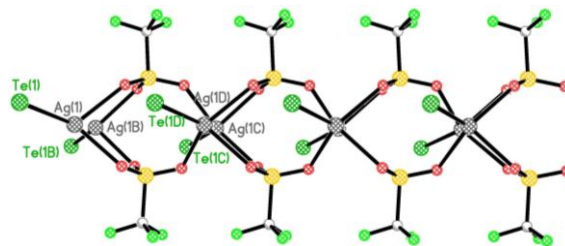

Fig. 16 The central coordination channel of **6** constructed from Ag, S and O atoms showing the bridging triflate anions.

Repeating (Ag$_2$OTf$_2$**L3**$_2$)$_n$ units, connected by the network of bridging triflate anions, extend along the y-axis to form 1D chains (Figures 14, 16). The central coordination channel made up of Ag, S and O atoms which dominates the extended lattice (Figure 16), is constructed around a single helical chain; silver centres are linked by O-S-O bridges from identical triflate molecules to form a left-handed helix [(-Ag(1)-O(3)-S(1)-O(2)-Ag(1)-O(1)-S(1)-O(2)-Ag(1)-)$_n$; Figure 17]. Additionally, as a consequence of the symmetry, each Ag$_2$OTf$_2$**L3**$_2$ unit combines to form symmetrical 8-membered macrocycles (Ag$_2$S$_2$O$_4$) which stack along the direction of the coordination channel.
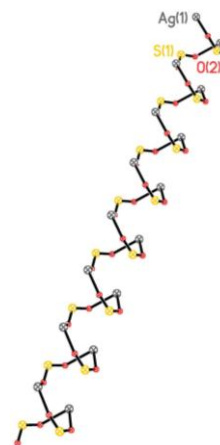

Fig. 17 The left-handed helix [(-Ag(1)-O(3)-S(1)-O(2)-Ag(1)-O(1)-S(1)-O(2)-Ag(1)-)$_n$] running through polymeric chain **6**

Extra stabilisation within each helical chain is provided by a number of weak intermolecular interactions; neighbouring acenaphthene fragments are connected by CH···π and CBr···π interactions whilst short CH···O and CH···F contacts link triflate anions to the organic backbone. Neighbouring helical chains extend parallel along the y-axis (Figure 18) and are connected by weak CH···π bonds between neighbouring acenaphthene fragments.

Looking down the extended chain polymer, the silver(I) ions align in two columns with the closest Ag···Ag distance 3.542(1) Å, slightly longer than twice the van der Waals radii of silver (3.44 Å).[24] Unsurprisingly the geometry of the acenaphthene fragment in **6** is unaffected by coordination within the helical chain. The equatorial arrangement positions the Te-C$_{Ph}$ bond

close to the acenaphthene plane,[25] with no apparent change in the molecular distortion compared with the free ligand **L3** [Te(1)···Br(1) 3.222(3) Å; *cf.* **L3** 3.2503(14) Å].[20]
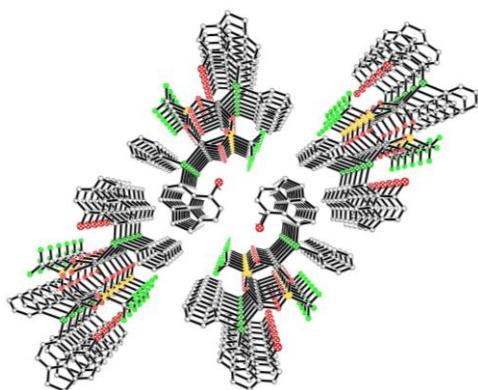

Fig. 18 View of the 1D extended helical chain polymer **6** along the y-axis (H atoms omitted for clarity).

Experimental Section

All experiments were carried out under an oxygen- and moisture-free nitrogen atmosphere using standard Schlenk techniques and glassware. Reagents were obtained from commercial sources and used as received. Dry solvents were collected from a MBraun solvent system. Elemental analyses were performed by Stephen Boyer at the London Metropolitan University. Infra-red spectra were recorded as KBr discs in the range 4000-300 cm^{-1} on a Perkin-Elmer System 2000 Fourier transform spectrometer. ^{1}H and ^{13}C NMR spectra were recorded on a Jeol GSX 270 MHz spectrometer with δ(H) and δ(C) referenced to external tetramethylsilane. ^{77}Se and ^{125}Te NMR spectra were recorded on a Jeol GSX 270 MHz spectrometer with δ(Se) and δ(Te) referenced to external dimethylselenide and diphenyl ditelluride respectively. ^{19}F NMR spectra were recorded on a Bruker Oxford 300 MHz spectrometer with δ(F) referenced to external trichlorofluoromethane. Assignments of ^{13}C and ^{1}H NMR spectra were made with the help of H-H COSY and HSQC experiments. All measurements were performed at 25 °C. All values reported for NMR spectroscopy are in parts per million (ppm). Coupling constants (*J*) are given in Hertz (Hz). Mass spectrometry was performed for **1, 2** and **4** by the University of St. Andrews Mass Spectrometry Service; Electrospray Mass Spectrometry (ESMS) was carried out on a Micromass LCT orthogonal accelerator time of flight mass spectrometer. Mass spectrometry was performed for **3, 5** and **6** by the EPSRC National Mass Spectrometry Service in Swansea.

[AgBF$_4${AcenapBr(SPh)}$_2$] (1): To a solution of silver tetrafluoroborate (0.18 g, 0.92 mmol) in dichloromethane (10 mL) was added a dichloromethane solution (20 mL) of 5-bromo-6-(phenylsulfanyl)acenaphthene (0.31 g, 0.92 mmol) at -30 °C. The reaction mixture was stirred at this temperature for 3 h and then at room temperature for a further 12 h affording a cloudy solution. The crude product was collected by filtration. An analytically pure sample was obtained by recrystallization from diffusion of hexane into a saturated dichloromethane solution of the product in the absence of light (0.19 g, 47%); mp 155-157 °C (decomp); elemental analysis (Found C, 49.3; H, 2.9. Calc. for

C$_{36}$H$_{26}$AgBBr$_2$F$_4$S$_2$: C, 49.4; H, 3.0 %); IR (KBr disk): ν_{max} cm^{-1}: 3407w, 3059w, 2922w, 2827w, 1871w, 1802w, 1743w, 1695w, 1655w, 1598s, 1577s, 1478s, 1439s, 1417s, 1404s, 1320s, 1258s, 1231s, 1204s, 1185w, 1132vs, 1085vs, 1025vs, 935s, 854s, 840s, 813s, 765w, 750vs, 734s, 687s, 623s, 605s, 560w, 519s, 507s, 467s, 398w, 356w, 310w; δ$_H$(270 MHz, (CD$_3$)$_2$CO, 25 °C, Me$_4$Si) 7.80 (2 H, d, $^3J_{HH}$ 7.4, 2 x Acenap 4-H), 7.68 (2 H, d, $^3J_{HH}$ 7.3, 2 x Acenap 7-H), 7.40-7.16 (14 H, m, 2 x Acenap 3,8-H, 2 x S*Ph* 12-16-H), 3.44-3.29 (8 H, m, 4 x C*H$_2$*); δ$_C$(67.9 MHz, (CD$_3$)$_2$CO, 25 °C, Me$_4$Si) 151.1(q), 149.1(q), 143.2(q), 139.5(s), 138.3(q), 137.1(s), 130.8(s), 130.7(q), 128.4(s), 125.9(q), 122.8(s), 122.2(s), 114.7(q), 31.2(s, 2 x C*H$_2$*), 31.0(s, 2 x C*H$_2$*); δ$_F$(376.5 MHz, (CD$_3$)$_2$CO, 25 °C, CCl$_3$F) -152.1(br s, ^{10}BF$_4^-$), -152.2(br s, ^{11}BF$_4^-$); MS (ES$^+$): *m/z* 790.63 (M$^+$-BF$_4^-$, 100%).

[AgBF$_4${AcenapBr(SePh)}$_2$] (2): To a solution of silver tetrafluoroborate (0.13 g, 0.65 mmol) in dichloromethane (20 mL) was added 5-bromo-6-(phenylselanyl)acenaphthene (0.25 g, 0.65 mmol) in one batch at -30 °C. The reaction mixture was stirred at this temperature for 3 h and then at room temperature for a further 12 h. The solvent was removed *in vacuo* affording a white precipitate. An analytically pure sample was obtained by recrystallization from diffusion of hexane into a saturated acetone solution of the product in the absence of light (0.26 g, 82%); mp 145-147 °C (decomp); elemental analysis (Found C, 44.5; H, 2.6. Calc. for C$_{36}$H$_{26}$AgBBr$_2$F$_4$Se$_2$: C, 44.5; H, 2.7 %); IR (KBr disk): ν_{max} cm^{-1}: 3420w, 3048w, 2923w, 2831w, 2143w, 1874w, 1849w, 1653w, 1599s, 1575s, 1561s, 1474s, 1436s, 1414s, 1347w, 1324s, 1301w, 1255w, 1231s, 1211w, 1082vs, 1054vs, 837vs, 810s, 742vs, 686s, 597w, 533w, 519s, 472s, 311w; δ$_H$(270 MHz, (CD$_3$)$_2$CO, 25 °C, Me$_4$Si) 7.75 (2 H, d, $^3J_{HH}$ 7.4, 2 x Acenap 4-H), 7.66-7.55 (4 H, m, 2 x Se*Ph* 12,16-H), 7.53-7.36 (6 H, m, 2 x Se*Ph* 13-15-H), 7.24-7.12 (4 H, m, 2 x Acenap 3,7-H), 7.07 (2 H, d, $^3J_{HH}$ 7.3, 2 x Acenap 8-H), 3.36-3.20 (8 H, m, 4 x C*H$_2$*); δ$_C$(67.9 MHz, (CD$_3$)$_2$CO, 25 °C, Me$_4$Si) 147.8(q), 147.5(q), 142.0(q), 135.6(s), 134.8(s), 133.3(s), 130.3(s), 129.9(q), 129.5(q), 129.4(s), 124.1(q), 121.4(s), 121.2(s), 114.2(q), 29.9(s, 2 x C*H$_2$*), 29.8(s, 2 x C*H$_2$*); δ$_{Se}$(51.5 MHz, (CD$_3$)$_2$CO, 25 °C, PhSeSePh) 390.6(s); δ$_F$(376.5 MHz, (CD$_3$)$_2$CO, 25 °C, CCl$_3$F) -152.1(br s, ^{10}BF$_4^-$), -152.2(br s, ^{11}BF$_4^-$); MS (ES$^+$): *m/z* 884.94 (M$^+$-BF$_4^-$, 100%).

[AgBF$_4${Acenap(Br)(TePh)}$_2$] (3): To a solution of silver tetrafluoroborate (0.08 g, 0.39 mmol) in dichloromethane (20 mL) was added 5-bromo-6-(phenyltelluro)acenaphthene (0.17 g, 0.39 mmol) in one batch at -30 °C. The reaction mixture was stirred at this temperature for 3 h and then at room temperature for a further 12 h. The solvent was removed *in vacuo* affording a white precipitate. An analytically pure sample was obtained by recrystallization from diffusion of hexane into a saturated dichloromethane solution of the product in the absence of light (0.17 g, 82%); mp 205-207 °C (decomp); elemental analysis (Found C, 40.3; H, 2.5. Calc. for C$_{36}$H$_{26}$AgBBr$_2$F$_4$Te$_2$: C, 40.5; H, 2.5 %); IR (KBr disk): ν_{max} cm^{-1}: 3422w, 3051w, 2923w, 2829w, 1875w, 1811w, 1648w, 1595s, 1558w, 1474w, 1435s, 1417s, 1325s, 1284w, 1256w, 1230w, 1212w, 1078vs, 1053vs, 1011vs, 839s, 809s, 764w, 742vs, 686s, 630s, 595w, 536w, 519w, 493w, 454w, 354w; δ$_H$(270 MHz, (CD$_3$)$_2$CO, 25 °C,

Me$_4$Si) 8.02-7.91 (2 H, m, Te*Ph* 12,16-H), 7.71 (1 H, d, $^3J_{HH}$ 7.5, Acenap 4-H), 7.62-7.45 (1 H, m, Te*Ph* 14-H), 7.45-7.34 (2 H, m, Te*Ph* 13,15-H), 7.20 (1 H, d, $^3J_{HH}$ 7.5, Acenap 3-H), 7.16 (1 H, d, $^3J_{HH}$ 7.6, Acenap 7-H), 7.02 (1 H, d, $^3J_{HH}$ 7.6, Acenap 8-H), 3.28-3.17 (4 H, m, 2 x C*H$_2$*); δ_C(67.9 MHz, (CD$_3$)$_2$CO, 25 ℃, Me$_4$Si) 142.0(s), 137.9(s), 133.4(s), 132.1(s), 131.9(s), 123.1(s), 123.0(s), 29.6(s, *CH$_2$*), 29.3(s,*CH$_2$*); δ_{Te}(81.2 MHz, (CD$_3$)$_2$CO, 25 ℃, PhTeTePh) 562.0(s); δ_F(376.5 MHz, (CD$_3$)$_2$CO, 25 ℃, CCl$_3$F) -152.1(br s, ^{10}BF$_4^-$), -152.2(br s, ^{11}BF$_4^-$); MS (ES$^+$): *m/z* 982.75 (M$^+$-BF$_4^-$, 100%).

[AgCF$_3$SO$_3${AcenapBr(SPh)}$_3$] (4): To a solution of silver trifluoromethanesulfonate (0.21 g, 0.81 mmol) in dichloromethane (10 mL) was added a dichloromethane solution (20 mL) of 5-bromo-6-(phenylsulfanyl)acenaphthene (0.28 g, 0.81 mmol) at -30 ℃. The reaction mixture was stirred at this temperature for 3 h and then at room temperature for a further 12 h affording a cloudy solution. The crude product was collected by filtration. An analytically pure sample was obtained by recrystallization from diffusion of hexane into a saturated dichloromethane solution of the product in the absence of light (0.32 g, 92%); mp 165-167 ℃ (decomp); IR (KBr disk): v_{max} cm^{-1}: 3442w, 3071w, 3054w, 3005w, 2927w, 2882w, 2835w, 2432w, 2346w, 2259w, 2202w, 1936w, 1873w, 1789w, 1729w, 1669w, 1639w, 1598s, 1580s, 1479s, 1439s, 1409s, 1323vs, 1264vs, 1172vs, 1114s, 1079s, 1028vs, 899s, 864s, 844vs, 815s, 763w, 735vs, 688s, 633vs, 577s, 517vs, 493s, 469s, 409w, 349w, 323w; δ_H(270 MHz, (CD$_3$)$_2$CO, 25 ℃, Me$_4$Si) 7.79 (3 H, d, $^3J_{HH}$ 7.4, 3 x Acenap 4-H), 7.65 (3 H, d, $^3J_{HH}$ 7.3, 3 x Acenap 7-H), 7.36-7.17 (15 H, m, 3 x Acenap 3,8-H, 3 x S*Ph* 13-15-H), 7.17-7.07 (6 H, m, 3 x S*Ph* 12,16-H), 3.44-3.30 (12 H, m, 6 x C*H$_2$*); δ_C(67.9 MHz, (CD$_3$)$_2$CO, 25 ℃, Me$_4$Si) 149.3(q), 147.8(q), 142.0(q), 139.0(q), 138.5(s), 135.8(s), 129.9(q), 129.4(s), 128.9(s), 126.3(s), 125.7(q), 121.4(s), 120.9(s), 113.8(q), 30.0(s, 3 x *CH$_2$*), 29.8(s, 3 x *CH$_2$*); δ_F(376.5 MHz, (CD$_3$)$_2$CO, 25 ℃, CCl$_3$F) -79.3(s); MS (ES$^+$): *m/z* 1302.73 (M$^+$+Na, 5%), 1046.8 (M$^+$+Na-AgOTf, 15), 788.76 (M$^+$-{Acenap(Br)(SPh)(OTf)}, 100).

[AgCF$_3$SO$_3${AcenapBr(SePh)}$_2$] (5): To a solution of silver trifluoromethanesulfonate (0.14 g, 0.70 mmol) in dichloromethane (10 mL) was added a dichloromethane solution (20 mL) of 5-bromo-6-(phenylselanyl)acenaphthene (0.27 g, 0.70 mmol) at -30 ℃. The reaction mixture was stirred at this temperature for 3 h and then at room temperature for a further 12 h. The reaction mixture was filtered and the solvent was removed *in vacuo* affording a brown precipitate. An analytically pure sample was obtained by recrystallization from diffusion of hexane into a saturated acetone solution of the product in the absence of light (0.22 g, 61%); mp 130-132 ℃ (decomp); elemental analysis (Found C, 42.9; H, 2.4. Calc. for C$_{37}$H$_{26}$AgBr$_2$F$_3$O$_3$SSe$_2$: C, 43.0; H, 2.5 %); IR (KBr disk): v_{max} cm^{-1}: 3423w, 3069w, 2929w, 2833w, 2231w, 1952w, 1858w, 1749w, 1652w, 1597s, 1575s, 1561s, 1473w, 1437s, 1411s, 1348w, 1327s, 1291vs, 1254vs, 1234vs, 1215vs, 1158vs, 1108s, 1065w, 1019vs, 935w, 912w, 837vs, 810s, 739vs, 687s, 633vs, 601s, 570w, 514s, 472w, 356w, 312w; δ_H(270 MHz, (CD$_3$)$_2$CO, 25 ℃, Me$_4$Si) 7.62 (2 H, d, $^3J_{HH}$ 7.4, 2 x Acenap 4-H), 7.60-7.51 (4 H, m, 2 x Se*Ph* 12,16-H), 7.43-7.27 (6 H, m, 2 x Se*Ph* 13-15-

H), 7.15-7.03 (4 H, m, 2 x Acenap 3,7-H), 6.98 (2 H, d, $^3J_{HH}$ 7.4, 2 x Acenap 8-H), 3.20-3.11 (8 H, m, 4 x C*H$_2$*); δ_H(67.9 MHz, (CD$_3$)$_2$CO, 25 ℃, Me$_4$Si) 149.0(q), 148.9(q), 143.2(q), 137.4(q), 136.9(s), 136.0(s), 134.7(s), 131.5(s), 130.9(q), 130.8(s), 122.6(s), 122.4(s), 115.6(q), 115.3(q), 29.3(s, 2 x *CH$_2$*), 29.0(s, 2 x *CH$_2$*); δ_{Se}(51.5 MHz, (CD$_3$)$_2$CO, 25 ℃, PhSeSePh) 387.8(s); δ_F(376.5 MHz, (CD$_3$)$_2$CO, 25 ℃, CCl$_3$F) -79.2(s); MS (ES$^+$): *m/z* 884.77 (M$^+$-OTf, 100%).

[AgCF$_3$SO$_3${Acenap(Br)(TePh)}] (6): To a solution of silver trifluoromethanesulfonate (0.11 g, 0.44 mmol) in dichloromethane (10 mL) was added a dichloromethane solution (20 mL) of 5-bromo-6-(phenyltelluro)acenaphthene (0.19 g, 0.44 mmol) at -30 ℃. The reaction mixture was stirred at this temperature for 3 h and then at room temperature for a further 12 h affording a cloudy solution. The crude product was collected by filtration. An analytically pure sample was obtained by recrystallization from diffusion of hexane into a saturated tetrahydrofuran solution of the product in the absence of light (0.28 g, 92%); mp 158-160 ℃ (decomp); elemental analysis (Found C, 32.9; H, 1.9. Calc. for C$_{19}$H$_{13}$AgBrF$_3$O$_3$STe: C, 32.9; H, 1.9 %); IR (KBr disk): v_{max} cm^{-1}: 1332w, 1249vs, 1225vs, 1176vs, 1106s, 1064w, 1031vs, 994s, 913w, 842s, 815s, 765w, 733s, 689s, 633vs, 600w, 579s, 517vs, 467w, 452w, 420w, 398w, 354w, 323w; δ_H(270 MHz, CD$_3$CN, 25 ℃, Me$_4$Si) 7.92-7.78 (2 H, m, Te*Ph* 12,16-H), 7.69 (1 H, d, $^3J_{HH}$ 7.4, Acenap 4-H), 7.62-7.51 (1 H, m, Te*Ph* 14-H), 7.48-7.34 (2 H, m, Te*Ph* 13,15-H), 7.16 (1 H, d, $^3J_{HH}$ = 7.4, Acenap 3-H), 7.07 (1 H, d, $^3J_{HH}$ = 7.4, Acenap 7-H), 6.94 (1 H, d, $^3J_{HH}$ 7.4, Acenap 8-H), 3.34-3.15 (4 H, m, 2 x C*H$_2$*); δ_C(67.9 MHz, CD$_3$CN, 25 ℃, Me$_4$Si) 148.2(q), 148.0(q), 141.6(q), 140.0(s), 135.6(s), 133.6(s), 130.9(q), 130.2(s), 130.0(s), 122.9(q), 121.2(s), 121.0(s), 114.9(q), 106.9(q), 29.2(s, *CH$_2$*), 29.1(s, *CH$_2$*); δ_{Te}(81.2 MHz, CD$_3$CN, 25 ℃, PhTeTePh) 559.0(s); δ_F(376.5 MHz, CD$_3$CN, 25 ℃, CCl$_3$F) -79.7(s); MS (ES$^+$): *m/z* 544.8 (M$^+$-OTf, 100%).

Crystal structure analyses

X-ray crystal structures for **1**-**3** and **6** were determined at -148(1) °C on the St Andrews Robotic Diffractometer[27] a Rigaku ACTOR-SM, Saturn 724 CCD area detector with graphite monochromated Mo-Kα radiation (λ = 0.71073 Å). The data was corrected for Lorentz, polarisation and absorption. Data for compounds **4** and **5** were collected at -180(1) °C by using a Rigaku MM007 High brilliance RA generator (Mo Kα radiation, confocal optic) and Saturn CCD system. At least a full hemisphere of data was collected using ω scans. Intensities were corrected for Lorentz, polarisation and absorption. The data for the complexes analysed was collected and processed using CrystalClear (Rigaku).[28] The structures were solved by direct methods[29] and expanded using Fourier techniques.[30] The non-hydrogen atoms were refined anisotropically. Hydrogen atoms were refined using the riding model. All calculations were performed using the CrystalStructure[31] crystallographic software package except for refinement, which was performed using SHELXL-97.[32] These X-ray data can be obtained free of charge via www.ccdc.cam.ac.uk/conts/retrieving.html or from the Cambridge Crystallographic Data centre, 12 Union Road, Cambridge CB2 1EZ, UK; fax (+44) 1223-336-033; e-mail:

Conclusions

The self-assembly of chalcogen-donor acenaphthenes [Acenap(Br)(EPh)] (Acenap = acenaphthene-5,6-diyl; E = S, Se, Te) **L1**-**L3**[20] with silver(I) salts, AgBF$_4$ and AgOTf, afforded six distinct silver(I) coordination complexes **1**-**6**, including two rare examples of organo-telluride silver(I) coordination. In each compound, the organic acenaphthene ligand (**L1**-**L3**) adopts the same ligation mode, binding to silver via classical monodentate coordination through the chalcogen atom. Nevertheless, modification of the chalcogen congeners within the ligand shell and the coordinating ability of the respective counter-anion affects the geometry adopted by the silver centre (linear, bent, trigonal planar, tetrahedral) and the structure of the final complex, generating two, three and four coordinate monomeric, mononuclear silver(I) complexes **1**-**5** and 1D polymeric chain **6**.

Independent reactions of the three chalcogen ligands **L1**-**L3** with AgBF$_4$ afforded three monomeric, mononuclear two-coordinate complexes. In each case, the BF$_4^-$ anion was shown to be non-coordinating, although weak intermolecular Ag···F interactions were observed. In the sulfur derivative **1**, silver adopts a bent coordination geometry, with neighbouring molecules associating to form dimers centred on an Ag$_2$F$_2$ rhombus core. Introduction of the heavier chalcogen congeners in the isomorphous complexes **2** and **3**, resulted in a linear metal geometry, with additional weak Ag···Br contacts constructing a *quasi*-chelate ring between the ligand and the silver centre in a distorted see-saw arrangement.

In contrast, the strong coordinating ability of the triflate anion affords two related monomeric three- (**5**) and four-coordinate (**4**) complexes and a 1D extended polymeric chain **6**. In each case, the triflate binds to silver via monodentate coordination through a single O atom, with additional weak Ag···O contacts in **6** affording a *quasi*-tetra-monodentate μ_4-bridging mode. The four-coordinate complex **4** is constructed from three sulfur **L1** ligands and a single triflate molecule, generating a tetrahedral environment around the central silver atom. In complex **5**, the additional bulk of the selenium ligand reduces the coordination, resulting in only two **L2** ligands and a triflate ion around the trigonal pyramidal silver. The mononuclear 1D polymeric chain **6** is assembled from repeating (Ag$_2$OTf$_2$**L3**$_2$)$_n$ units, linked by a network of μ_4-bridging triflate anions. The central coordination channel within the extended lattice is constructed from secondary silver-triflate interactions and contains a single left-handed helix [(-Ag(1)-O(3)-S(1)-O(2)-Ag(1)-O(1)-S(1)-O(2)-Ag(1)-)$_n$].

Acknowledgements

Notes and references

^{a} School of Chemistry, University of St Andrews, St Andrews, Fife, U.K. Fax: (+44) 1334 463384; Tel: (+44)1334 463861; E-mail: jdw3@st-andrews.ac.uk, frk@st-andrews.ac.uk

1 D. Venkataraman, Y. Du, S. R. Wilson, K. A. Hirsch, P. Zhang and J. S. Moore, *J. Chem. Educ.,* 1997, **74**, 915.

2 a) C.-T. Chen and K. S. Suslick, *Coord. Chem. Rev.,* 1993, **128**, 293; b) M. Fujita, Y. J. Kwon, S. Washizu and K. Ogura, *J. Am. Chem. Soc.,* 1994, **116**, 1151; c) B. F. Hoskins and R. Robson, *J. Am. Chem. Soc.,* 1990, **112**, 1546.

3 a) L. Carlucci, G. Ciani, D. M. Proserpio and A. Sironi, *J. Am. Chem. Soc.,* 1995, **117**, 4562; b) G. B. Gardner, D. Venkataraman, J. S. Moore and S. Lee, *Nature*, 1995, **374**, 792.

4 a) B. Li, S.-Q. Zang, R. Liang, Y.-J. Wu and T. C. W. Mak, *Organometallics*, 2011, **30**, 1710; b) J.-R. Li, X.-He. Bu, J. Jiao, W.-P. Du, X.-H. Xu and R.-H. Zhang, *Dalton Trans.,* 2005, 464; c) C.-K. Tan, J. Wang, J.-D. Leng, L.-L. Zheng and M.-L. Tong, *Eur. J. Inorg. Chem.,* 2008, 771.

5 a) A. D. Burrows, D. J. Kelly, M. F. Mahon, P. R. Raithby, C. Richardson and A. J. Stevenson, *Dalton Trans.,* 2011, **40**, 5483; b) X.-H. Bu, W. Chen, W.-F.Hou, M. Du, R.-H. Zhang and F. Brisse, *Inorg. Chem.,* 2002, **41**, 3477; c) J.-R. Li, R.-H. Zhang and X.-H. Bu, *J. Chem. Crystallogr.,* 2004, **34**, 501.

6 C.-K. Tan, J. Wang, J.-D. Leng, L.-L. Zheng and M.-L. Tong, *Eur. J. Inorg. Chem.,* 2008, 771.

7 D. G. Booth, W. Levason, J. J. Quirk, G. Reid and S. M. Smith, *Dalton Trans.,* 1997, 3493.

8 A. G. Young and L. R. Hanton, *Coord. Chem. Rev.,* 2008, **252**, 1346.

9 I. Ino, L. P. Wu, M. Munakata, M. Maekawa, Y. Suenaga, T. Kuroda-Sowa and Y. Kitamori, *Inorg Chem.,* 2000, **39**, 2146.

10 P. L. Caradoc-Davies and L. R. Hanton, *Chem. Commun.*, 2001, 1098.

11 a) C. A. Coulson, R. Daudel and J. M. Robertson, *Proc. R. Soc. London Ser. A*., 1951, **207**, 306; b) D. W. Cruickshank, *Acta Crystallogr.,* 1957, **10**, 504; c) C. P. Brock and J. D. Dunitz, *Acta Crystallogr., Sect. B*, 1982, **38**, 2218; d) J. Oddershede and S. Larsen, *J. Phys. Chem. A,* 2004, **108**, 1057.

12 A. C. Hazell, R. G. Hazell, L. Norskov-Lauritsen, C. E. Briant and D. W. Jones, *Acta Crystallogr., Sect. C,* 1986, **42**, 690.

13 a) P. Kilian, F. R. Knight and J. D. Woollins, *Chem. Eur. J*., 2011, **17**, 2302; b) P. Kilian, F. R. Knight and J. D. Woollins, *Coord. Chem. Rev*., 2011, **255**, 1387.

14 V. Balasubramaniyan, *Chem. Rev*., 1966, **66**, 567.

15 a) S. M. Aucott, H. L. Milton, S. D. Robertson, A. M. Z. Slawin, G. D. Walker and J. D. Woollins, *Chem. Eur. J.,* 2004, **10**, 1666: b) S. M. Aucott, H. L. Milton, S. D. Robertson, A. M. Z. Slawin and J. D. Woollins, *Heteroat. Chem.,* 2004, **15**, 531; c) S. M. Aucott, H. L. Milton, S. D. Robertson, A. M. Z. Slawin and J. D. Woollins, *Dalton Trans.*, 2004, 3347: d) S. M. Aucott, P. Kilian, H. L. Milton, S. D. Robertson, A. M. Z. Slawin and J. D. Woollins, *Inorg. Chem.,* 2005, **44**, 2710; e) S. M. Aucott, P. Kilian, S. D. Robertson, A. M. Z. Slawin and J. D. Woollins, *Chem. Eur. J.,* 2006, **12**, 895: f) S. M. Aucott, D. Duerden, Y. Li, A. M. Z. Slawin, J. D. Woollins, *Chem. Eur. J.,* 2006, **12**, 5495.

16 a) P. Kilian, A. M. Z. Slawin and J. D. Woollins, *Dalton Trans*., 2003, 3876; b) P. Kilian, D. Philp, A. M. Z. Slawin and J. D. Woollins, *Eur. J. Inorg. Chem.,* 2003, 249: c) P. Kilian, A. M. Z. Slawin and J. D. Woollins, *Chem. Eur. J.,* 2003, **9**, 215; d) P. Kilian, A. M. Z. Slawin and J. D. Woollins, *Chem. Commun.,* 2003, 1174; e) P. Kilian, H. L. Milton A. M. Z. Slawin and J. D. Woollins, *Inorg. Chem.,* 2004, **43**, 2252; f) P. Kilian, A. M. Z. Slawin and J. D.

Woollins, *Inorg. Chim. Acta,* 2005, **358**, 1719; g) P. Kilian, A. M. Z. Slawin and J. D. Woollins, *Dalton Trans.*, 2006, 2175.

17 a) F. R. Knight, A. L. Fuller, A. M. Z. Slawin and J. D. Woollins, *Dalton Trans.*, 2009, 8476; b) F. R. Knight, A. L. Fuller, A. M. Z. Slawin and J. D. Woollins, *Polyhedron,* 2010, **29**, 1849; c) F. R. Knight, A. L. Fuller, A. M. Z. Slawin and J. D. Woollins, *Polyhedron,* 2010, **29**, 1956; d) F. R. Knight, A. L. Fuller, M. Bühl, A. M. Z. Slawin, J. D. Woollins, *Chem. Eur. J.*, 2010, **16**, 7617.

18 a) F. R. Knight, A. L. Fuller, M. Bühl, A. M. Z. Slawin and J. D. Woollins, *Chem. Eur. J.,* 2010, **16**, 7503; b) A. L. Fuller, F. R. Knight, A. M. Z. Slawin and J. D. Woollins, *Eur. J. Inorg. Chem.,* 2010, 4034; c) F. R. Knight, A. L. Fuller, M. Bühl, A. M. Z. Slawin and J. D. Woollins, *Inorg. Chem.,* 2010, **49**, 7577; d) F. R. Knight, A. L. Fuller, M. Bühl, A. M. Z. Slawin and J. D. Woollins, *Chem. Eur. J.,* 2010, **16**, 7605; e) A. L. Fuller, F. R. Knight, A. M. Z. Slawin and J. D. Woollins, *Acta Crystallogr., Sect. E,* 2007, **E63**, o3855; f) A. L. Fuller, F. R. Knight, A. M. Z. Slawin and J. D. Woollins, *Acta Crystallogr., Sect. E,* 2007, **E63**, o3957; g) A. L. Fuller, F. R. Knight, A. M. Z. Slawin and J. D. Woollins, *Acta Crystallogr., Sect. E,* 2008, **E64**, o977.

19 M.-L. Lechner, K. S. Athukorala Arachchige, R. A. M. Randall, F. R. Knight, M. Bühl, A. M. Z. Slawin and J. D. Woollins, *Organometallics,* 2012, **31**, 2922.

20 a) L. K. Aschenbach, F. R. Knight, R. A. M. Randall, D. B. Cordes, A. Baggott, M. Bühl, A. M. Z. Slawin and J. D. Woollins, *Dalton Trans.,* 2012, **41**, 3141; b) F. R. Knight, K. S. Athukorala Arachchige, R. A. M. Randall, M. Bühl, A. M. Z. Slawin and J. D. Woollins, *Dalton Trans.,* 2012, **41**, 3154.

21 F. R. Knight, R. A. M. Randall, L. Wakefield, A. M. Z. Slawin and J. D. Woollins, *Inorg. Chem.*, 2012, submitted.

22 F. H. Allen, J. E. Davies, J. J. Galloy, O. Johnson, O. Kennard, C. F. Macrae, E. M. Mitchell, G. F. Mitchell, J. M. Smith and D. G. Watson, *J. Chem. Inf. Comput. Sci.,* 1991, **31**, 187.

23 a) W. Levason, M. Nirwan, R. Ratnani, G. Reid, N. Tsoureas and M. Webster, *Dalton Trans.,* 2007, 439; b) W. Levason, G. Reid and V.-A. Tolhurst, *J. Chem. Soc., Dalton Trans.,* 1998, 3411; c) K. Kobayashi, H. Masu, A. Shuto and K. Yamaguchi, *Chem. Mater.,* 2005, **17**, 6666; d) W. Levason, S. D. Orchard and G. Reid, *Chem. Commun.,* 2001, 427; e) W.-F. Liaw, C.-H. Lai, S.-J. Chiou, Y.-C. Horng, C.-C. Chou, M.-C. Liaw, G.-H. Lee and S.-M. Peng, *Inorg. Chem.,* 1995, **34**, 3755.

24 A. Bondi, *J. Phys. Chem.*, 1964, **68**, 441.

25 P. Nagy, D. Szabó, I. Kapovits, Á. Kucsman, G. Argay and A. Kálmán, *J. Mol. Struct*., 2002, **606**, 61.

26 a) W. Nakanishi, S. Hayashi and S. Toyota, *Chem. Commun*., 1996, 371; b) W. Nakanishi, S. Hayashi, A. Sakaue, G. Ono and Y. Kawada, *J. Am. Chem. Soc*., 1998, **120**, 3635; c) W. Nakanishi, S. Hayashi and S. Toyota, *J. Org. Chem*., 1998, **63**, 8790; d) S. Hayashi and W. Nakanishi, *J. Org. Chem*., 1999, **64**, 6688; e) W. Nakanishi, S. Hayashi and T. Uehara, *J. Phys. Chem. A,* 1999, **103**, 9906; f) W. Nakanishi, S. Hayashi and T. Uehara, *Eur. J. Org. Chem.,* 2001, 3933; g) W. Nakanishi and S. Hayashi, *Phosphorus Sulfur Silicon Relat. Elem.,* 2002, **177**, 1833; h) W. Nakanishi, S. Hayashi and T. Arai, *Chem. Commun.,* 2002, 2416; i) S. Hayashi and W. Nakanishi, *J. Org. Chem.,* 2002, **67**, 38; j) W. Nakanishi, S. Hayashi and N. Itoh, *Chem. Commun.,* 2003, 124; k) S. Hayashi, H. Wada, T. Ueno and W. Nakanishi, *J. Org. Chem.,* 2006, **71**, 5574; l) S. Hayashi and W. Nakanishi, *Bull. Chem. Soc. Jpn.,* 2008, **81**, 1605.

27 A. L. Fuller, L. A. S. Scott-Hayward, Y. Li, M. Bühl, A. M. Z. Slawin and J. D. Woollins*, J. Am. Chem. Soc.,* 2010, **132**, 5799.

28 CrystalClear 1.6: Rigaku Corporation, 1999. CrystalClear Software User's Guide, Molecular Structure Corporation, (c) 2000. J. W. P. Flugrath, *Acta Crystallogr., Sect. D,* 1999, **D55**, 1718.

29 SIR97: A. Altomare, M. Burla, M. Camalli, G. Cascarano, C. Giacovazzo, A. Guagliardi, A. Moliterni, G. Polidori and R. Spagna, *J. Appl. Cryst*., 1999, **32**, 115.

30 DIRDIF99: P. T. Beurskens, G. Admiraal, G. Beurskens, W. P. Bosman, R. de Gelder, R. Israel, J. M. M. Smits, 1999. The DIRDIF-99 program system, Technical Report of the Crystallography Laboratory, University of Nijmegen, The Netherlands.

31 CrystalStructure 3.8.1: Crystal Structure Analysis Package, Rigaku and Rigaku/MSC (2000-2006). 9009 New Trails Dr. The Woodlands TX 77381 USA.

32 SHELX97: G. M. Sheldrick, *Acta Crystallogr., Sect. A,* 2008, **64**, 112.